Complexation of the anti-*Trypanosoma cruzi* Drug Benznidazole Improves Solubility and Efficacy

Jean Jerley Nogueira Silva,[†] Wander Rogério Pavanelli,[‡] Fredy R. Salazar Gutierrez,[‡] Francisco Chagas Alves Lima,[†] Albérico Borges Ferreira da Silva,[†] João Santana Silva,[‡] and Douglas Wagner Franco*[,†]

Departamento de Química e Física Molecular, Instituto de Química de São Carlos, Universidade de São Paulo (USP), São Carlos, SP, Brazil, Departamento de Bioquímica e Imunologia, Faculdade de Medicina de Ribeirão Preto, Universidade de São Paulo (USP), Ribeirão Preto, SP, Brazil

Received October 17, 2007

The ruthenium complex, *trans*-[Ru(Bz)$(NH_3)_4SO_2](CF_3SO_3)_2$ **1**, Bz = benznidazole (*N*-benzyl-2-(2-nitro-1*H*-imidazol-1-yl)acetamide), is more hydrosoluble and more active ($IC_{50try/1\ h} = 79 \pm 3\ \mu M$) than free benznidazole **2** ($IC_{50try/1\ h} > 1$ mM). **1** also exhibits low acute toxicity in vitro ($IC_{50macrophages} > 1$ mM) and in vivo (400 μmol/kg < LD_{50} < 600 μmol/kg) and the formation of hydroxylamine is more favorable in **1** than in **2** by 9.6 kcal/mol. In murine acute models of Chagas' disease, **1** was more active than **2** even when only one dose was administrated. Moreover, **1** at a thousand-fold smaller concentration than the considered optimal dose for **2** (385 μmol/kg/day = 100 mg/kg/day), proved to be sufficient to protect all infected mice, eliminating the amastigotes in their hearts and skeletal muscles as observed in H&E micrographics.

Introduction

American trypanosomiasis or Chagas' disease (ChD)[a] remains a significant public health problem and is still one of the major causes of morbidity and mortality from cardiovascular diseases in Latin America despite nearly one century of research.[1] The American Red Cross has recently published a study showing that one in 4655 blood donors in the United States was confirmed as positive for *T. cruzi* antibodies.[2] Furthermore, actions for preventing transmission of *T. cruzi* infection by organ transplant or blood transfusion have also been taken in nonendemic areas such as the European countries,[3] thus showing that this disease is a cause for concern to developed countries as well.[3]

Despite the progress achieved in the study of *T. cruzi*'s biochemistry and physiology in which several enzymes have been identified as potential new targets, a definitive chemotherapy for this parasitic infection remains undeveloped.[4,5] The compounds benznidazole **2** (Bz), (*N*-benzyl-2-(2-nitro-1*H*-imidazol-1-yl)acetamide) and gentian violet **3** (Gv), (*N*-[4-(bis[4-(dimethylamino)-phenyl]methylene]-2,5-cyclohaxadien-1-ylidene]-*N*-methyl-methanaminium chloride) are only clinically used for the treatment of ChD and blood sterilization, respectively. However, the Bz treatment is unsatisfactory and exhibit undesirable side effects such as anorexia, dermatotoxicity, digestive disorders, peripheral polyneuropathy, genotoxicity, and allergic dermopathy attributed to the redox damage to the host's tissue.[6–10] If administrated in the acute phase, **2** could cure 50−70% of the patients, but a very low cure rate (8−20%) was reported for chronically infected patients even when treated for more than 10 years.[6] Furthermore, several strains of *T. cruzi* (e.g., Y, Colombiana, CS-28, and VL-10) are naturally Bz-resistant.[11] **2** is claimed to act through the formation of free radicals and/or electrophilic metabolites.[9] The nitro group in **2** is reduced to an amino group through the nitroreductases, and this process begins with a reaction catalyzed by NADPH-cytochrome P-450 reductase, producing a nitro anion radical ($R\text{-}NO_2^{\bullet -}$),[9] which is involved in its trypanocidal effect by covalent bonding to macromolecules such as the DNA parasite.[9]

More recently, efforts have been devoted to the synthesis and evaluation of platinum, palladium, rhenium, copper, gold, and ruthenium derivatives as trypanocidal drugs.[12–14] However, these metal complexes have limited pharmacological application due to their low hydrosolubility and toxic effects.[12–15] An interesting series of ruthenium complexes,[14,15] type $[Ru(H_2O)_2L_2](PF_6)_2$, $[RuL_2Cl_2]$, $[RuL_3Cl_3]\cdot 2CH_3OH$, $[RuL_2(H_2O)Cl_3]\cdot 2H_2O$, and $[Ru(bpy)L_2](PF_6)_2$, L = clotrimazole (Ctz) or ketoconazole (Ktz) less toxic than the ones mentioned above, has been used in the rational design of new antiparasitic agents. This species can block specific lipid biosynthesis pathways by, e.g., inhibiting the enzyme cytochrome P450 14α-demethylase involved in the production of ergoesterol, which are essential for the parasite.[12,14,15] According to the authors,[14,15] these ruthenium complexes are able to inhibit 70% of proliferation of epimastigote forms of *T. cruzi*.[12] Furthermore, the ruthenium complexes $[Ru(Ctz)_2(H_2O)_2](PF_6)_2$ and $[Ru(Ktz)_2(H_2O)Cl_3]$ acting in synergism with antifungal drugs have proved to be more active than the corresponding free ligands.[14,15]

Following this approach, the $[Ru(NH_3)_4L]^{n+}$ moiety has been successfully tested as NO carrier in vitro and in vivo[16,17] because the NO production has been ascribed as a responsible for the

* To whom correspondence should be addressed. Phone: +55 16 3373 9976. Fax: +55 16 3373 9976. E-mail: douglas@iqsc.usp.br. Address: Av. Trabalhador São-Carlense, 400 CP 780, 13560-970 São Carlos, SP, Brazil. This paper is based on part of the J. J. N. Silva, Ph.D. Thesis and is presented as the Brazilian patent of invention PI 0704577-8.

[†] Departamento de Química e Física Molecular, Instituto de Química de São Carlos, Universidade de São Paulo.

[‡] Departamento de Bioquímica e Imunologia, Faculdade de Medicina de Ribeirão Preto, Universidade de São Paulo.

[a] Abbreviations: BT, bloodstream trypomastigote forms of *Trypanosoma cruzi*; Bz, benznidazole; ChD, Chagas' disease; DFT, density functional theory; E_{aq}, total energy in aqueous phase; E_s, solvation energy; ΔE_{NO2}, difference in reduction potential of NO_2 moiety between **1** and **2**; GAP = $E_{LUMO} - E_{HOMO}$; $IC_{50try/1\ h}$, inhibitory concentration on trypomastigote forms after 1 h incubation; $IC_{50try/4\ h}$, inhibitory concentration on trypomastigote forms after 4 h incubation; $IC_{50try/24\ h}$, inhibitory concentration on trypomastigote forms after 24 h incubation; MLCT, metal-to-ligand charge-transfer transition; MO, molecular orbital; NBO, natural bond orbital analysis; PBS, phosphate-buffered saline; Protocol A, treatment for 15 consecutive days; Protocol B, treatment only on the fifth, sixth, and seventh days preceding the parasitaemic peak; S_{aq}, water solubility; SCE, aqueous saturated calomel electrode; % TA, percentage of trypanocidal activity; *T. cruzi*, *Trypanosoma cruzi*.

10.1021/jm701306r CCC: $40.75
Published on Web 06/21/2008

Scheme 1. General Procedures Used to Prepare the Desired Complex Ion **1**[a]

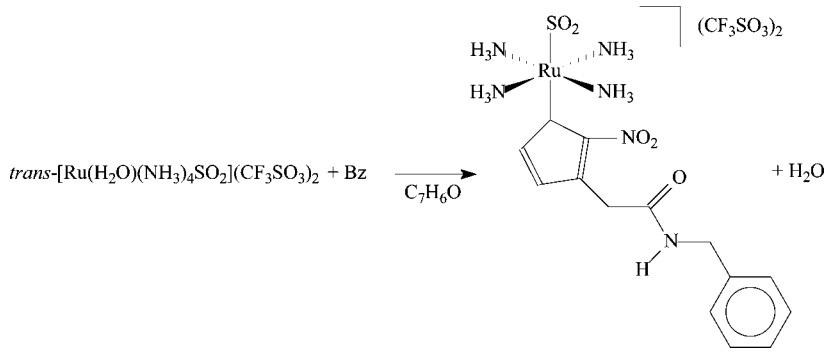

[a] The precursor complex ion was prepared according to the literature.[19]

trypanocidal effect in activated macrophages.[18] In fact, in a recent related work, *trans*-$[Ru(NO)(NH_3)_4L]^{n+}$, L = *N*-heterocyclic, SO_3^{2-}, or $P(OEt)_3$ exhibited not only low cytotoxicity but also anti-*T. cruzi* activity due to NO action.[17]

In this context, ruthenium(II) tetraammine compounds are good models for tailoring carriers for Bz because these species are water soluble due to the presence of the NH_3 ligands and readily react with *N*-heretocyclic ligands yielding quite robust compounds.[19–21] Moreover, it is likely that these complexes, upon coordination to the Bz, shift the reduction potential of the nitro group in **2** to more positive values, benefiting the formation of the corresponding nitro radical anion and subsequent hydroxylamine derivative. Because activity of **2** is attributed to the generations of reduced metabolites, which are involved in its trypanocidal effects,[22] it is expected that the RuBz complex, which the Bz ligand would be more accessible to reduction, exhibits higher anti-*T. cruzi* activity than free Bz.

Using this general strategy and aiming to develop a more water soluble and more active anti-*T. cruzi* compound with reduced toxicity, we describe here the *trans*-$[Ru(Bz)(NH_3)_4SO_2](CF_3SO_3)_2$ complex **1**, where Bz = benznidazole, which in biological media yields *trans*-$[Ru(Bz)(NH_3)_4SO_3]$. Assays of acute toxicity for **1** were then evaluated on female Swiss mice, and comparison of the trypanocidal activity in vitro and in vivo of **1** and **2** was performed using a partially Bz-resistant strain. Results are explained based on both experimental and theoretical parameters and the Ru(II) moiety influence on the chemical properties of Bz ligand.[19,20]

Results

Chemistry. The New Ruthenium Complex, *trans*-$[Ru(Bz)(NH_3)_4SO_2](CF_3HSO_3)_2$. The first experiments were carried out with $[Ru(H_2O)(NH_3)_5](PF_6)_2$ complex and **2** in acetone. As predicted from the redox potentials of Ru(III)/Ru(II) couple in the aquopentaamine ruthenium species[23] and of the nitro group in **2**,[24] a redox reaction leading to metal center oxidation was observed. The chemical reactivity of Ru(II) center is attributed to its strong back-bonding ability in the binding to unsaturated ligands.[19–21] Because of the π acidity of the sulfur atom in SO_2, HSO_3^-, and SO_3^{2-} ligands, the Ru(II) center in the *trans*-$[Ru(H_2O)(NH_3)_4SO_2]^{2+}$ complex ion becomes a weaker reductant agent than in $[Ru(H_2O)(NH_3)_5]^{2+}$. It is well-known that the substitution of one of the NH_3 ligands by SO_2 in $[Ru(NH_3)_5Cl]^{2+}$ complex ion yields a well-defined and less reductant species (Scheme 1) than in $[Ru(H_2O)(NH_3)_5]^{2+}$.[19,20,25] Furthermore, the *trans* labilizing and *trans* influence effects of SO_2 increase the lability of the *trans* aquo ligand in *trans*-$[Ru(H_2O)(NH_3)_4SO_2]^{2+}$, facilitating their substitution by entering ligands such as **2**.[26] Additionally, through *cis* delabilizing effect of SO_2 ligand, NH_3 equatorial ligands still become more inert regarding the substitution reactions,[19,27] thus resulting in the predictable quite robust *trans*-$[Ru(Bz)(NH_3)_4SO_2]^{2+}$ complex ion **1** (Scheme 1).[19,28] Compound **1** was isolated as *trans*-$[Ru(Bz)(NH_3)_4SO_2](CF_3HSO_3)_2$ from the reaction between *trans*-$[Ru(H_2O)(NH_3)_4SO_2]^{2+}$ and **2** in acetone and characterized by elemental analyses, spectroscopic techniques (^1H and ^{13}C NMR, IR, and UV−vis), and density functional theory (DFT) calculations.

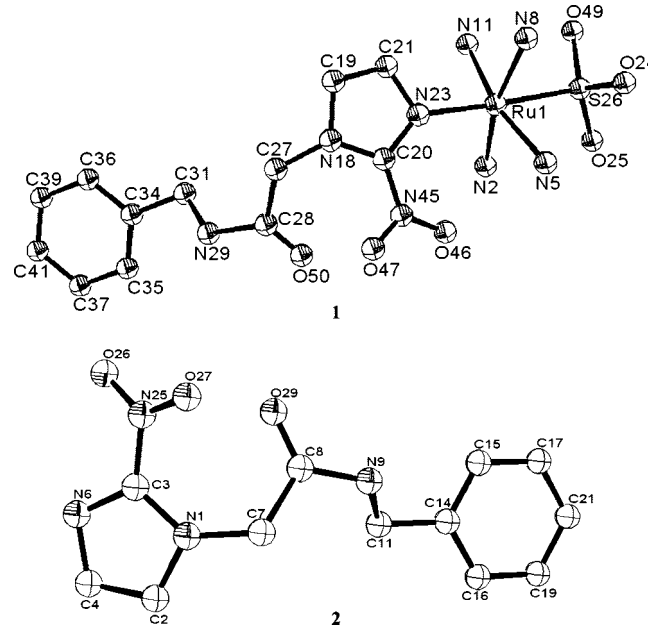

Figure 1. Optimized structure for *trans*-$[Ru(Bz)(NH_3)_4(SO_3)]$ **1** and structure of the currently used drug for the treatment of ChD, benznidazole **2**. Both compounds were optimized by ab initio DFT calculations in aqueous phase.

Structural Analysis. So far it has not been possible to obtain a good crystal for complex **1**. Therefore, a structural analysis was performed using an optimized geometry calculated through DFT (Figure 1). The main objective was to evaluate the bond lengths Ru−NH_3, Ru−N(Bz), and Ru−S, and the angles H_3N−Ru−NH_3 and O−S−O. Ru−N interatomic distance for the equatorial ammines does not change significantly when L is SO_2 (2.182 Å), HSO_3^- (2.194 Å), or SO_3^{2-} (2.201 Å). However, this is not true for Ru−N(Bz) bond distance considering 2.151, 2.106, and 2.072 Å for L = SO_2, HSO_3^-, or SO_3^{2-}, respectively. Thus, Ru−N(Bz) bond strengthening is observed when L = SO_2, HSO_3^-, or SO_3^{2-}, respectively, which is

consistent with the simultaneous Ru−S weakening, thus reflecting the increase of the biphilic character of L ligand. Additionally, $H_3N-Ru-NH_3$ (90.1 ± 1.2) and O−S−O (116.6 ± 2.5) angles are approximately the same as in *trans*-$[Ru(NH_3)_4SO_2Cl]Cl$.[28]

Molecular Orbital Analysis. The molecular orbital (MO) composition of **1** was performed considering L = SO_2 representing the isolated species. LUMO and the two empty MOs LUMO + 2 and LUMO + 3 have a combination of SO_2 ligands orbitals (20−40%), Bz antibonding orbitals (11–55%), and ruthenium dσ orbitals (16−49%). However, the empty MO LUMO + 1 has 100% Bz antibonding character centered in the imN-NO_2 moiety. In the same way, instead of a single HOMO, there are three close-lying highest occupied orbitals, which have a combination of ruthenium (3%), SO_2 (10%), and Bz (87%) orbitals for HOMO, 100% Bz phenyl group for HOMO-1 and HOMO-2, and 100% ruthenium dπ orbital for HOMO-3. Their energies would be ∼2.7 eV below the set of π^* orbitals of the Bz imidazole ring. Therefore, in addition to intraligand band (n → π^*) in the ultraviolet region,[29] a metal-to-ligand charge-transfer (MLCT) transition (Ru → Bz) in the visible region (approximately 470−500 nm ≅ 2.5 eV) is also predicted. According to time-dependent DFT (TD-DFT) calculations, this transition would be spin forbidden and would occur nearly 540 nm (∼2.3 eV) with low intensity (oscillator strength (f) = 5.5 × 10^{-3}).

Electronic Absorption Spectra. UV−vis spectra of **1** were recorded in water, ethanol, and acetone. Spectrum of **2** in ethanol shows an intraligand band at 314 nm, $\varepsilon = 8.2 \times 10^3$ M^{-1} cm^{-1} ascribed to n → π^* transition.[29] This same transition, upon coordination to Ru(II) center, is shifted to 323 nm, $\varepsilon = 8.1 \times 10^3$ $M^{-1}cm^{-1}$ and 322 nm, $\varepsilon = 4.5 \times 10^3$ M^{-1} cm^{-1} in ethanol and water, respectively. The spectrum of **1** in acetone, ethanol, and water exhibits a second band at 477 nm, $\varepsilon = 71$ M^{-1} cm^{-1}, 507 nm, $\varepsilon = 89$ M^{-1} cm^{-1}, and at 530 nm, $\varepsilon = 84$ M^{-1} cm^{-1}, respectively, which, according to the DFT calculations, could be assigned as MLCT. According to MO composition for **1**, HOMO-3 has 100% Ru_{dyz} character, whereas LUMO + 1 has 100% imN-$NO_{2px\pi^*}$ character. Although this transition has small intensity due to the asymmetry of the orbitals, it shows solvatochromism (C_3H_6O, λ_{abs} = 477 nm; C_2H_6O, λ_{abs} = 507 nm; H_2O, λ_{abs} = 530 nm), which would suggest a charge-transfer character. Thus, the experimental data for the electronic spectrum are on agreement with DFT calculations predictions.

Vibrational Frequencies. The infrared absorption bands νNO_2, 1371 cm^{-1}, νCN, 1523 cm^{-1}, and νCO, 1633 cm^{-1} for **1** are coherent, with the Bz axial coordination to R(II) center through N_{23} unsubstantiated nitrogen atom (Figure 1). These frequencies were shifted to smaller values, considering the free ligand, upon coordination. As previously mentioned, DFT calculations suggest that the back-bonding Ru(II)−N(Bz) involves the ruthenium d_{yz} orbitals (100% Ru_{dyz}, HOMO-3) and the imidazole ring π^* orbitals in Bz (100% imN−NO_{2px} π^*, LUMO + 1). Therefore, it is expected that, upon coordination, bonds of the imidazole ring become weaker and, consequently, these frequencies are shifted to smaller wavenumbers. Furthermore, the infrared absorption bands νSO_{2sym} = 1107 cm^{-1} and νSO_{2asym} = 1281 and 1249 cm^{-1} are consistent with the SO_2 ligand coordination through sulfur atom, as in *trans*-$[Ru(NH_3)_4SO_2Cl]Cl$.[28]

NMR Spectra. Compound **1** was also well characterized by ^1H and ^{13}C NMR spectroscopy. A small ^1H shift considering the free ligand was observed for H_{21} ($\Delta\delta$ 0.09) and H_{19} ($\Delta\delta$ 0.05) atoms located in the vicinity of the coordinated nitrogen.

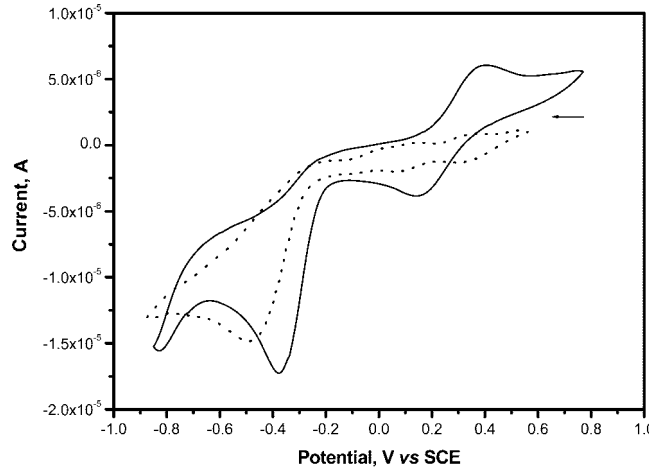

Figure 2. Cyclic voltammograms for **1** (—) and **2** (---) in a protic media (NaTFA, 0.1M, pH = 2.2). υ = 100 mV/s. Cathodic wave corresponding to the hydroxylamine formation from NO_2 moiety according to Bz-NO_2 + 4e + 4H → Bz-NHOH + H_2O.

Correspondingly, a small ^{13}C shift considering the free ligand was observed for C_{20} ($\Delta\delta$ 0.73) and C_{21} ($\Delta\delta$ 0.34) atoms, as expected for Ru−N(Bz) bond.[29] All other protons and carbons shifted by <0.1 ppm. Additionally, the carbonyl group of **1** was detected in ^{13}C resonance (δ167.3), and the ammonia ligand and ammine group detected in ^1H resonance at δ3.1 and δ7.9, respectively.

Cyclic Voltammetry. Comparison of cyclic voltammetry data of both the ruthenium species and the ligand itself was used to reveal the formation of the corresponding hydroxylamine derivative, which is the stable product of the electrochemical nitro reduction of **2** in protic medium.[24] **2** exhibits an irreversible cathodic wave at −0.475 V vs SCE (pH = 2.2) attributed to a four-electron and four-proton transfer to form the hydroxylamine derivate.[24]

$$Bz-NO_2 + 4\bar{e} + 4H^+ \rightarrow Bz-NHOH + H_2O \qquad (1)$$

After coordination, under the same conditions, this reduction wave was shifted by +0.104 V, benefiting the formation of the nitroanion radical and subsequent hydroxylamine by 9.6 kcal/mol. Furthermore, a reversible redox couple with $E_{1/2}$ = 0.273 V vs SCE was also observed and ascribed to Ru(III)/Ru(II) couple (Figure 2).

Titration of 1 by Alkali. From the titration of compound **1** with NaOH (Figure 3), two pK_a values can be determined corresponding to the equilibria:

trans-$[Ru(Bz)(NH_3)_4(SO_2)]^{2+}$ +

$$2H_2O \rightleftharpoons \textit{trans}\text{-}[Ru(Bz)(NH_3)_4(HSO_3)]^+ + H_3O^+ \quad pK_{a1} = 1.2 \pm 0.1$$

trans-$[Ru(Bz)(NH_3)_4(HSO_3)]^+$ +

$$H_2O \rightleftharpoons \textit{trans}\text{-}[Ru(Bz)(NH_3)_4(SO_3)]^+ + H_3O^+ \quad pK_{a2} = 4.3 \pm 0.1$$

These values are smaller than the ones reported[19] for the *trans*-$[Ru(H_2O)(NH_3)_4(SO_2)]^{2+}$ and *trans*-$[Ru(H_2O)(NH_3)_4(HSO_3)]^+$, which are 2.1 and 5.0, respectively. This is coherent with the higher basicity of Bz in relation to H_2O and the consequent increase of the electron density along the ruthenium−sulfur axis. Indeed, this has been anticipated by DFT calculations.

As it can be observed in Figure 3, at physiological pH, the *trans*-$[Ru(Bz)(NH_3)_4SO_3]$ species is the predominant form of **1**.

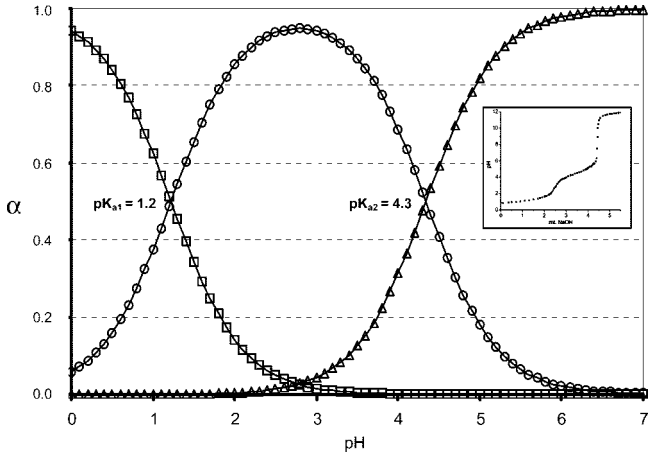

Figure 3. Distribution of *trans*-$[Ru(Bz)(NH_3)_4L]^{2+/+/0}$, L = SO_2 (square), HSO_3^- (circle), or SO_3^{2-} (triangle) species as a function of hydrogen concentrations and titration curve (inside) with NaOH at 25 °C.

Hydrophilic and Electronic Properties. Differences in the hydrophilic and electronic properties between **1** and **2** were analyzed through DFT calculations considering L = SO_3^{2-}, the predominant form for **1** in physiological medium. The molecular properties determined and examined in this study were LUMO energy, GAP ($E_{LUMO} - E_{HOMO}$), total energy in aqueous phase (E_{aq}), solvation energy in water (E_s), and atomic charges obtained by using the natural bond orbital analysis (NBO) method.[7,8] Table 1 summarizes the main electronic and hydrophilic differences between **1** and **2**. As predicted,[22,24] electrochemical reduction can occur in the nitro group because this moiety is the most susceptible part of **1** and **2** to nucleophilic attack. These data are also in agreement with the NBO charges calculated, showing that the NO_2 moiety is more electrophilic in **1** (N_{45}, 0.43; $O_{46/47}$, −0.32) than in **2** (N_{25}, 0.42; $O_{26/27}$, −0.37). Furthermore, according to GAP and LUMO energies, the electronic affinity of the nitro group in **1** would be higher than in **2** because the calculated energies in **1** (GAP = 1.85 eV) are smaller than in **2** (GAP = 2.54 eV)[7,8] (Table 1).

In agreement with the experimental data for hydrosolubity, the calculated solvation energy and total energy in aqueous phase have pointed out that **1** would be more water soluble than **2**. Whereas **2** is not highly soluble in water (0.4 mg/mL = 0.2 μmol/mL, at 37 °C),[30] the experimentally measured water solubility of **1** is 3.7 mg/mL = 4.4 μmol/mL in the same medium (Table 1).

Biology. Toxicity Assays. Cell viability was the experimental model used to evaluate cytotoxicity in vitro at concentrations of **1** ranging from 10 nM to 1 mM and using macrophages or spleen cells from Balb/c mice. Lymphocytes, which are the most abundant types of cells present in spleen cells, are a highly susceptible group of cells, and their proliferation depends on the interaction with viable macrophages. Because the concentrations assayed for **1** did not reduce the viability of macrophages or splenocytes, it is reasonable to assume that IC_{50} against macrophages is higher than those concentrations. Thus, considering the IC_{50try} = 79 μM and $IC_{50macrophages}$ > 1 mM for **1**, its in vitro therapeutic window (tw = $IC_{50macrophages}/IC_{50try}$) is higher than 12. According to the reported data,[33] the IC_{50} value for **2** on Chinese hamster lung fibroblasts (V-79 cells) is 2 mM. Therefore, its IC_{50} against trypomastigotes (IC_{50try} > 1 mM) is very proximal of the value against V-79 cells (2 mM), suggesting a quite narrow therapeutic window for **2**.

At concentrations up to 400 μmol/kg, no acute toxic effect was observed for **1** when using an up-and-down method in vivo.[34] However, at 600 μmol/kg concentrations, the mice died, thus suggesting that LD_{50} for **1** ranges between 400 and 600 μmol/kg.

In Vitro Trypanocidal Activity on Trypomastigotes. As expected,[35,36] **2** after 1 h of incubation at 37 °C at 1 mM concentrations presented very low percentage of lysis (<15%) of bloodstream trypomastigotes (BT) of the Y strain of *T. cruzi*. However, under the same conditions, **1** showed higher activity than **2** over this partially Bz-resistant strain, with %TA equal to 63 ± 7, 75 ± 4, 95 ± 6, and 100 (mean ± SEM, n = 4−7) at concentrations of 0.1, 0.25, 0.5, and 1.0 mM, respectively. Accordingly, **1** exhibits smaller inhibitory concentration ($IC_{50try/1\ h}$ = 79 ± 3 μM) than **2** ($IC_{50try/1\ h}$ > 1 mM) after 1 h of incubation (Table 1). Furthermore, when **1** is compared with the current blood sterilization drug **3**, $IC_{50try/24\ h}$ on BT for **1** ($IC_{50try/24\ h}$ = 58 ± 4 μM) is about 1 order of magnitude smaller than the value reported for **3** ($IC_{50try/24\ h}$ = 536 μM).[37]

In Vitro Antiproliferative Activity on Epimastigotes. Experiments carried out to determine the in vitro antiproliferative activity of compounds **1** and **2** were set up using cultures of epimastigote forms. Table 2 summarizes the antiproliferative activity data of these compounds in the exponential phase of *T. cruzi* growth expressed as the percentage of growth inhibition (% GI). According to these data, **1** is shown to exhibit greater antiproliferative activity (IC_{50epi} = 127 ± 8 μM) than **2** (IC_{50epi} > 1 mM) under the conditions tested.

In Vivo Trypanocidal Activity (Acute Model). Preliminary assays were conducted with *trans*-$[Ru(H_2O)(NH_3)_4SO_2]$-$(CF_3HSO_3)_2$ complex, a precursor in the synthesis of **1** (Scheme 1). No in vivo activity was observed for this compound when administrated in doses up to 350 μmol/kg for 15 consecutive days in *T. cruzi*-infected Swiss mice. After that, different in vivo murine models for acute ChD were used to compare the activity of compounds **1** and **2**. Groups of six female Swiss mice were inoculated and intraperitoneally treated for 15 consecutive days (protocol A) or for only three days, the fifth, sixth, and seventh days that precede the parasitaemic peak (protocol B) with doses of **1**. As Figure 4b shows, **1** at 100 nmol/kg dose provided good level of protection against death (60%) when mice were treated according to protocol A, whereas no protection was observed for the nontreated group, not even when treated with **2** at 100 nmol/kg dose for 15 consecutive days. Furthermore, the parasitemia levels were significantly smaller (P > 0.05) than the control group levels when mice were treated with **1** according to protocols A or B (Figure 4a).

With the purpose of comparison, other groups of mice were inoculated with 1.0 × 10^3 BT per mouse and orally treated with **1** at 100 nmol/kg and 385 nmol/kg and with **2** at 385 μmol/kg for 15 consecutive days. Note that **1** at 385 nmol/kg dose is a thousand-fold smaller than the considered optimal dose (385 μmol/kg = 100 mg/kg) for **2**.[38,39] Figure 5a shows that, similarly to the group intraperitoneally treated, **1** at 100 nmol/kg dose orally administrated also decreases the parasitaemic peak by 65−70%. As a consequence, this dose assured 60% survival of the treated animals (Figure 5b). However, when the infected mice were treated with either 385 nmol/kg dose of **1** or 385 μmol/kg dose of **2**, 100% survival was observed with a significant decrease (P > 0.001) of the parasitaemic peak for **1** and **2**. In another experiment, mice were inoculated with 1.0 × 10^3 BT per mouse and orally treated with **1** or **2** at 385 μmol/kg only on the first day after infection. While **1** was able to

Table 1. Comparison of in Vitro Activity and Molecular Electronic (LUMO Energy, NBO Charges) in Nitro Group, and Difference of Energy between the Frontier Orbital (GAP = $E_{LUMO} - E_{HOMO}$) and Hydrophilic (Solvation Energy, Total Energy in Aqueous Phase, and Water Solubility) Descriptors and E_{pc} for **1** and **2**

compounds	$IC_{50try/1\ h}$ (μM)	survival (%)[a]	LUMO (eV)	GAP[b] (eV)	NBO[c]	E_{pc} (V)[d]	E_{Aq} (kcal/mol)[e]	E_s (kcal/mol)[f]	S_{aq} (mg/mL)[g]
1	79 ± 3	60	−3.19	1.85	N_{45}(0.43), $O_{46/47}$ (−0.32)	−0.371	-1.61×10^6	−306.69	3.7
2	<1000	0	−3.94	2.54	N_{25}(0.42), $O_{26/27}$ (−0.37)	−0.475	-5.70×10^5	−8.21	0.4[30]

[a] % survival at 100 nmol/kg dose administrated (ip) for 15 consecutive days. [b] GAP = $E_{LUMO} - E_{HOMO}$ optimized by DFT calculations in aqueous phase considering L as SO_3^{2-}. [c] NBO: charges in nitro group. The charges in oxygen atom are the average between that of the nitro moiety. [d] E_{pc}: reduction potential according to reaction Bz-NO_2 + 4e + $4H^+$ → Bz-NHOH + H_2O, pH = 2.2, μ = 0.1 M of $NaCF_3COO$, potential versus SCE. [e] E_{aq}: total energy in aqueous phase considering L as SO_3^{2-}. [f] E_s: solvation energy in water considering L as SO_3^{2-}. [g] S_{aq}: experimental water solubility (pH = 6.5 and t = 37 °C).[52,53]

Table 2. Antiproliferative Activity of **1** and **2** on Epimastigote Forms at Different Concentrations and Incubation Times

	antiproliferative activity (% GI)									
	T = 1 h			T = 4 h			T = 24 h			
compounds	0.1[a]	0.5	1	0.1	0.5	1	0.1	0.5	1	IC_{50epi} (μm)
1	33 ± 5	56 ± 4	67 ± 3	63 ± 4	75 ± 4	80 ± 6	69 ± 6	79 ± 5	92 ± 3	127 ± 8
2	0	0	7 ± 3	11 ± 3	15 ± 4	24 ± 2	15 ± 4	26 ± 4	31 ± 5	>1000

[a] Values are express in mM. Results are mean ± SEM, n = 3, P < 0.05. Antiproliferative activity expressed as the percentage of growth inhibition at defined concentration. IC_{50epi} corresponding to 50% antiproliferative activity after 24 h incubation.

protect 60% of the infected animals, **2** was able to protect only 20% (data not shown).

Histological Analysis. Experiments have been performed according to a previously described protocol.[18,36] Swiss mice were intraperitoneally infected with 1.0×10^3 BT per mouse and treated with different doses of **1** and **2** for 15 consecutive days. On the 15th day after infection, all surviving mice from the nontreated group, the group intraperitoneally treated with **1** at 100 nmol/kg (Figure 4b), and the group orally treated with **1** at 100 nmol/kg, 385 nmol/kg and **2** at 385 μmol/kg (Figure 5b) were euthanized and their hearts (Figure 4c and 5c), skeletal muscles (Figure 4c), and livers (Figure 6) processed for H&E stain. Groups of uninfected mice were also euthanized and their organs processed for comparison.

Microscopic analysis revealed that infected and nontreated mice (control) showed several nests of amastigotes in their hearts as well as in their skeletal muscles, whereas mice treated with **1** at 100 nmol/kg dose showed no nests either in their hearts or in their skeletal muscles (Figure 4c). Furthermore, results obtained from these experiments have also showed that chemotherapy with **1** decreases the occurrence of myocarditis (Figure 4c and 5c). When considering the group treated with **2** at the same single dose as **1**, that is 385 μmol/kg, the nests of amastigotes in the mice's hearts were not completely eradicated for both of the compounds (data not shown). Figure 6 reveals that the group treated with **1** showed a smaller number of inflammatory cells in their livers than the group treated with **2**. Additionally, from liver histological analysis, no morphological evidence for toxicity was found when Swiss mice were treated with **1** at 385 nmol/kg for 15 consecutive days.

Discussion

Previous work[40,41] has shown that some ruthenium complexes transporting antifungal or semicarbazones are more active against *T. cruzi* than the corresponding free ligands. However, the low solubility of these complexes in water limits their pharmacology potential.[12] It has been reported that etanidazole (*N*-(2-hydroxyethyl)-2-nitro-1-imidazoleacetamide), a new 2-nitroimidazole used as a clinical hypoxic cell radiosensitizer, displays trypanocidal activity against isolated trypomastigotes and amastigotes of *T. cruzi* not affecting host cell viability. Although not completely equivalent to Bz, etanidazole takes advantage in exerting its anti-*T. cruzi* activity for longer periods with no serious toxic effects as those recorded for Bz-treated patients. According to this report,[42] the small toxic effects found for etanidazole were ascribed to its higher hydrosolubility than Bz. Similarly, active 2*H*-benzimidazole 1,3 dioxide derivatives are more hydrosoluble, electrophilic, and easily reduced than the inactive ones.[7] The presence of the NH_3 and SO_2 ligands, which make the complex **1** more soluble in water than **2**, has circumvented this inconvenience. Furthermore, as mentioned here before, at physiological pH, the *trans*-[Ru(Bz)$(NH_3)_4SO_3$] is the predominant form of **1**, a neutral species that also could be facilitate the complex movement across the cellular membranes.

It is well accepted that the biochemical mechanism of action of **2** involves reduction of the nitro group to a nitro radical anion as a key step.[9,22,43] The reduced intermediates do not stimulate redox cycling but act covalently, modifying biomacromolecules such as DNA or cytochrome P_{450} of the parasite.[9,44] Upon coordination, the nitro radical anion formation in **1** would become more easily accessible to nitroreductase enzymes because the cathodic wave attributed to reduction of the nitro group to the corresponding hydroxylamine derivative was shifted to −0.371 V vs SCE in acid medium. Therefore, the coordination of **2** to the $[Ru(NH_3)_4SO_2]^{2+}$ moiety will activate the NO_2 group toward reduction by +0.104 V favoring the nitro radical anion formation and subsequent hydroxylamine derivative by 9.6 kcal/mol in terms of free energy. Accordingly, the molecular electrostatic potential energy isosurfaces (MEP) and NBO charges show that the nitro group in **1** (N_{45}, 0.43; $O_{46/47}$, −0.32) is more electrophilic than in **2** (N_{25}, 0.42; $O_{26/27}$, −0.37), hence more susceptible to nucleophilic attack upon coordination to the Ru(II) center (Table 1). The difference of energy between the frontier orbitals (GAP = $E_{LUMO} - E_{HOMO}$) was claimed to be associated with the trypanocidal activity in pyrazolo pyridine and 5-ethenylbenzofuroxan derivatives.[45,46] The smaller the GAP value, the higher the electronic affinity in the electrophilic groups (e.g., NO_2 moiety) the more active are the compounds.[45,46] The GAP for **1**, optimized by DFT calculations in aqueous phase, is 1.85 eV, whereas for **2** the GAP is 2.54 eV. This GAP energy decrease is in agreement with the higher electronic

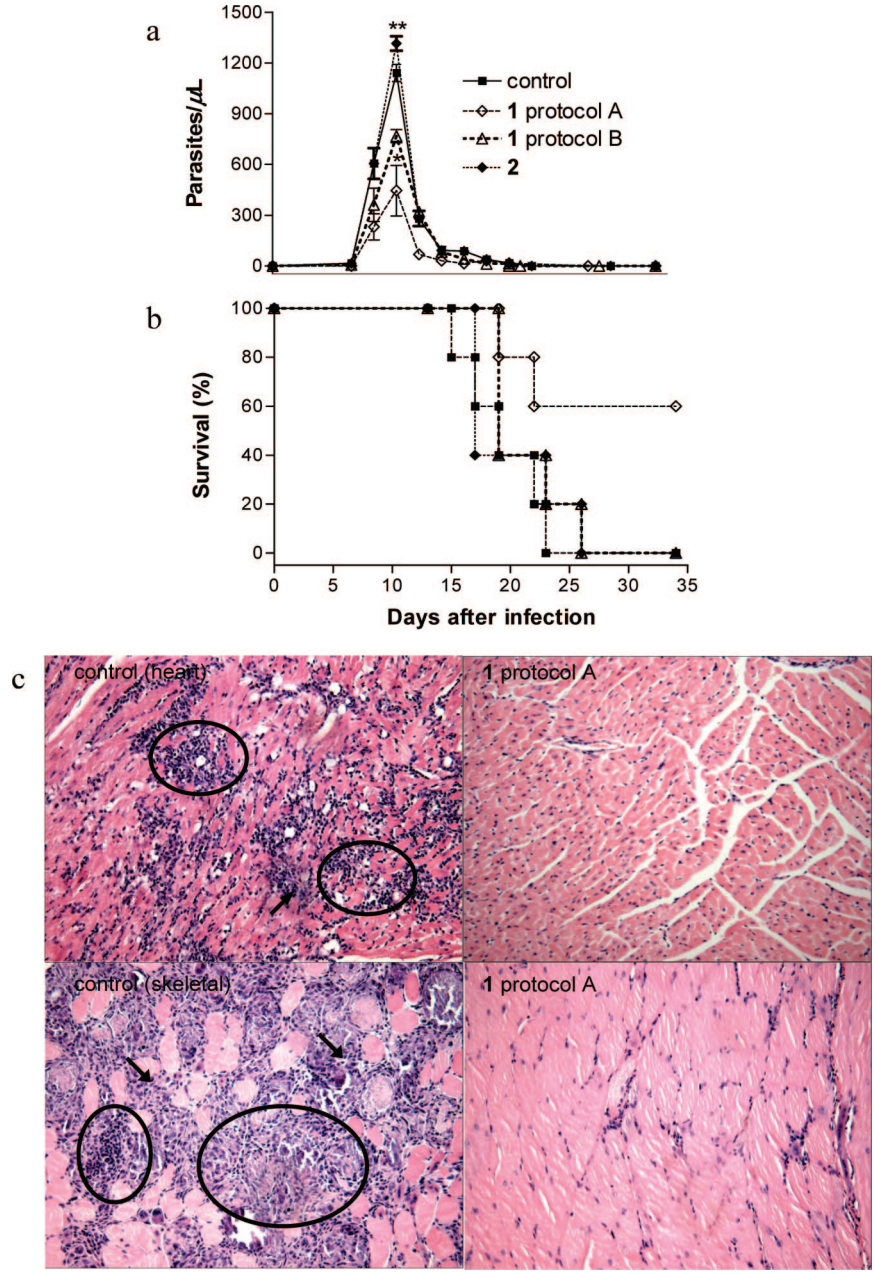

Figure 4. Parasitemia (a), survival rate (b), and representative microphotographs of heart (c) and skeletal muscle (d) sections of Swiss mice infected with *T. cruzi* and treated with **1** or **2**. Mice were infected with *T. cruzi* (Y strain, 1.0×10^3 BT per mouse) and treated with **1** at 100 nmol/kg for 15 consecutive days (protocol A, open diamond), or only on the 5th, 6th, and 7th days (protocol B, triangle). Other groups of infected mice received only PBS (control, square) or doses of **2** at 100 nmol/kg (closed diamond). 100 μL PBS were intraperitoneally administrated for all treatments. In a similar experiment, mice were euthanized on the 15th day after infection and their heart and skeletal muscles processed for H&E stain. Note the presence of amastigotes nests (arrows) and the intensity of the inflammatory process with mononuclear cell infiltrates (circles) in the control panels and no occurrence in the micrographics treated with **1** according to protocol A. Data are representative of three independent experiments with similar results, $n = 6$. Final magnification: 200×.

affinity of NO_2 moiety in **1** than in **2** and with the higher accessibility to the reduction potential of the nitro group (NO_2/$NO_2^{\bullet-}$) by nitroreductase enzymes (Figure 2, Table 1).[7,9,22] Thus, the best performance of **1** than **2** could be a consequence of a higher accessibility of the nitro group to reduction (Table 2).

Compound **1** administrated at 385 nmol/kg exhibits 100% protection against death when infected mice are treated for 15 consecutive days. It is important to remind that this dose is a thousand-fold smaller than the optimal dose for **2** (385 μmol/kg = 100 mg/kg).[36] The data presented here for **2** are also in agreement with those previously published, showing that it also exhibited 100% protection against death when infected mice were treated with a 385 μmol/kg dose for 20 consecutive days.[38] However, in this work, when infected mice were treated with **2** at 100 nmol/kg, no protection against death was observed, whereas mice treated with **1** showed 60% protection up to 120 days (Figure 4b). This indicates that this new benznidazole derivative **1** is more active than **2** even in concentrations 4000 times smaller than its data estimated in vivo acute toxicity ($LD_{50} > 400$ μmol/kg). Furthermore, **1** was also more active than **2** even when only one dose was administrated.

In Central and South America, the chronic phase of the ChD is one of the main causes of death due to heart failure.[47] In addition to being highly toxic, **2** exhibits a very low efficacy in

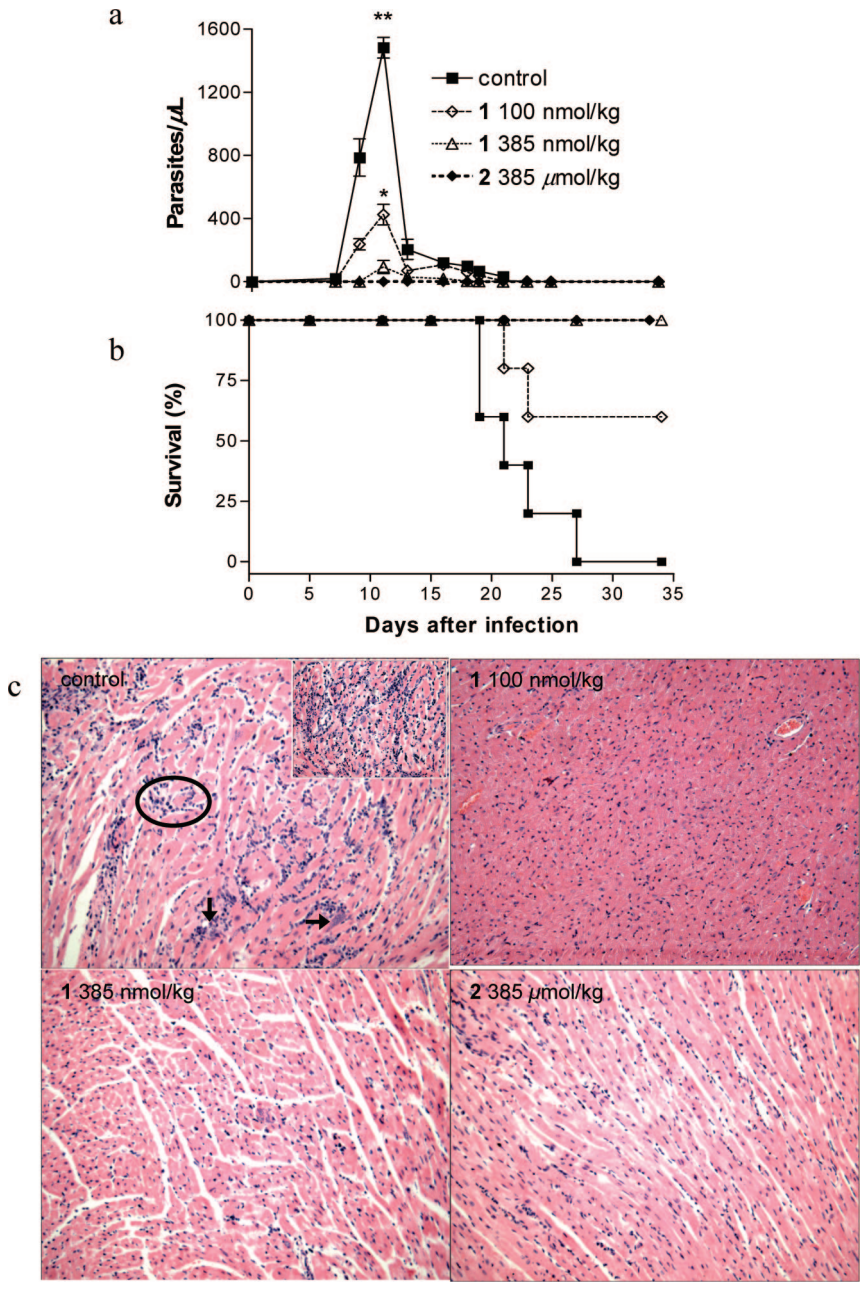

Figure 5. Parasitemia (a), survival rate (b), and representative microphotographs of heart (c) sections of Swiss mice infected with *T. cruzi* and treated with **1**, **2**, or nontreated (control). Mice were infected with *T. cruzi* (Y strain, 1.0×10^3 BT per mouse) and treated with **1** at 100 nmol/kg dose (open diamond), 385 nmol/kg (triangle), or with **2** 385 μmol/kg (closed diamond). Another group of infected mice was not treated (control, square). 100 μL of PBS were orally administrated for all treatments. In a similar experiment, mice were euthanized on the 15th day after infection and their hearts processed for H&E stain. Note the presence of amastigotes nests (arrows) and the intensity of the inflammatory process with mononuclear cell infiltrates (circles) in the nontreated group (control) and no occurrence in the micrographics treated with **1** at 100 nmol/kg, **1** at 385 nmol/kg, or **2** at 385 μmol/kg. 200 μL for **1** and 100 μL for **2** were orally administrated for all treatments. Data are representative of three independent experiments with similar results, $n = 6$. Final magnification: 200×.

the treatment of patients chronically infected with *T. cruzi*.[47,48] It has recently been reported that treatment of mice with **2** with a 385 μmol/kg dose prevents from severe chronic cardiomyophaty, but it does not lead to a complete parasite eradication.[47] On the other hand, **1** with a 100 nmol/kg dose proved to eliminate the nests of amastigotes in myocardium tissue and skeletal muscles and decrease myocarditis in the mouse acute model. In fact, preliminary experiments carried out to evaluate the trypanocidal activity of **1** on amastigotes-infected Vero cells showed that this compound is able to eliminate viable amastigotes inside the Vero cells (data not shown). This reinforces the potential therapeutic use of this compound as chemoprophylaxis as well as chemotherapeutic agents.

Conclusion

The new hydrosoluble ruthenium benznidazole derivative **1** reported here behaves as a promising anti-*T. cruzi* compound displaying interesting activities either in vitro or in vivo studies. The higher trypanocidal activity for compound **1** than **2** could be ascribed to the coordination of **2** to the *trans*-$[Ru(NH_3)_4L]^{2+/+/0}$ moiety. The potentialization of the benznidazole through coordination to the metal center can be explained based

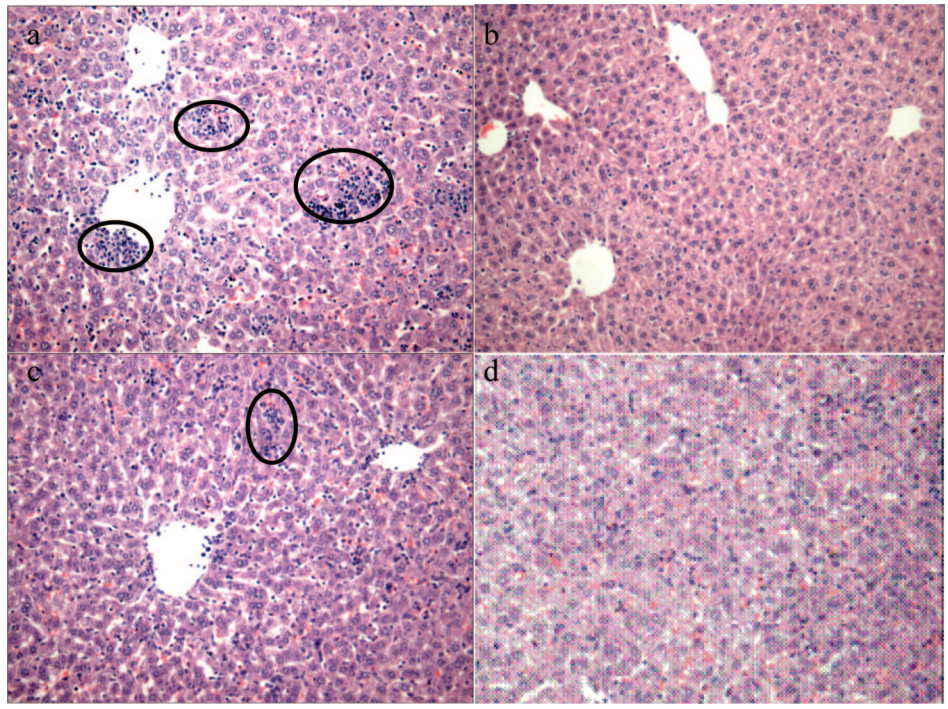

Figure 6. Representative microphotographs of liver sections of mice infected with *T. cruzi* 1.0×10^3 BT per mouse and nontreated group (a) or treated with **1** at 385 nmol/kg (b) or **2** at 385 μmol/kg (c). Panel (d) represents a liver from a noninfected group. 100 μL for **1** and 200 μL for **2** were orally administrated for all treatments. On the 15th day after infection, mice were euthanized and their livers processed for H&E stain. Circles indicate the inflammatory cells. Microphotographs are representative of three independent experiments with similar results, $n = 6$. Final magnification: 200×.

on the electron withdrawing ability of the Ru(II) center due to of the L ligand and the increase on the Bz water solubility promoted by the coordination to the quite hydrophilic *trans*-$[Ru(NH_3)_4L]^{2+/+/0}$ moiety. Furthermore, **1** does not exhibit any acute toxicity in Swiss mice at doses up to 400 μmol/kg. Assays to verify the activity of **1** on other pathogenic trypanosomatids such as *Leishimania major* are on course and results will be reported soon.

Experimental Section

Chemicals and Reagents. Ruthenium trichloride (Aldrich) was the starting material for the synthesis of all ruthenium complexes described herein. All solvents were purified following known procedures[49] and doubly distilled water was used throughout. All syntheses and manipulations were carried out under argon atmosphere.[50] **2** was obtained from Sigma-Aldrich and used as reference drug.

Ruthenium Complexes. The *trans*-$[Ru(H_2O)(NH_3)_4(SO_2)](TFMS)_2$ complex was synthesized and characterized following published procedures.[19,28] **1** was prepared by the reaction between the *trans*-$[Ru(H_2O)(NH_3)_4(SO_2)](TFMS)_2$ complex (35 mg, 64 μmol) and **2** (40 mg, 0.15 mmol) in degassed acetone. Upon 2 h of reaction, under argon atmosphere, the solution was rotevaporated and the pale-yellow solid collected, filtered inside of a glovebag, washed with 50 mL of degassed hexane three times, and kept in dessicator under vacuum. As suggested from electronic and infrared spectra, this complex is stable for at least 2 months when stored under these conditions. Yield better than 55%. Calcd for *trans*-$[Ru(Bz)(NH_3)_4(SO_2)](TFMS)_2 \cdot C_3H_6O$: H, 3.53; N, 13.19; C, 24.03; S, 11.32; Ru, 11.90. Found: H, 3.36; N, 13.32; C, 24.78; S, 11.06; Ru, 11.83. Thermogravimetric (TG) experiments were performed using a TGA-951 thermogravimetric unit coupled to a TGA-2100 thermal analyzer, both from TA Instruments, using a sample mass of ca. 7 mg and a platinum sample holder under 90 mL/min dynamic air flow. Only under temperatures higher than 218 °C was mass loss observed. Therefore, it is reasonable to assume that **1** has thermal stability under temperatures up to 200 °C.

Instrumentation. Hydrogen, carbon, nitrogen, and sulfur elemental microanalyses were done using an EA 1110 CHNS-O CE Instrument. Ruthenium analyses were performed according to the method proposed in published procedures,[51] using a Polarized Zeeman atomic absorption spectrophotometer, Z-8100 Hitachi, with a Hitachi hollow cathode lamp, 12 mA, and 349.9 nm wavelength.

UV−visible measurements were performed in a 1.0 cm quartz cell on a 8452A Hewlett-Packard diode array spectrophotometer. IR spectra were recorded on a MB-102 Bomem FTIR spectrophotometer at 400−4000 cm^{-1} range in KBr pellets (1 wt %). The ^1H and ^{13}C NMR spectra were performed in acetone-d_6 and recorded on a Bruker DPX-200 instruments at 200 MHz.

A 264A Princeton Applied Research polarographic analyzer/stripping voltammeter attached to a microcomputer and employing Microquímica Eletrochemical Software was used for the electrochemical measurements. The electrochemical cell used was a conventional three-electrode type with an aqueous saturated calomel electrode (SCE) as a reference electrode and a glassy-carbon and platinum wire as working and auxiliary electrodes, respectively. The solutions were degassed with argon for 10 min before each measurement at 25 °C.

Solubility Measurements. The solubility values for **1** were determined simulating a "bio-relevant" medium (pH = 6.5, t = 37 °C), which simulates the proximal small intestine in the fasted state. This medium was prepared as previously reported[52,53] and contained 3 mM sodium taurocholate, 0.75 mM lecithin, 3.9 mg KH_2PO_4, 7.7 mg KCl, and had regulated pH of 6.5−7.4 with NaOH. A known amount of **1** was added to 5 mL of the medium, and the resulting suspension was stirred for 24 h and filtered through a 0.45 μm filter. The filtered suspension was then diluted and assayed by UV−vis at 323nm ($\varepsilon = 4.5 \times 10^3$ M^{-1} cm^{-1}) to determine in triplicate[52,53] the concentration of **1**.

Titration of 1 by Alkali. The pK_a experiments were performed according to a previous report.[19] Then 25 mL of **1** was transferred to a cell holding a combination electrode. The titrating solution, NaOH 0.1 N, measured by means of a glass micrometer calibrated to read 0.05 mL, was conduced through a burette. The temperature was 25 ± 0.1 °C, measured during the experiment. Standard buffers

at pH 4.004, 7.006, and 10.008 (25.0 °C) were used to standardize the pH meter.

Molecular Descriptors. DFT calculations were performed using the Gaussian 03 program.[54] Optimized molecular geometries were obtained in vacuum by using the hybrid functional B3LYP,[55,56] the standard 6-31G(d) basis set for H, C, N, S, and O, and the LANL2DZ basis set for Ru. B3LYP includes the functional developed by Becke et al.,[55] which combines the Becke's gradient part of the exchange functional,[57] the Lee−Yang−Parr,[58] and the Vosko−Wilk−Nusair correlation functional with part of the exact Hartree−Fock exchange energy.[56] All the minimal energies were characterized by frequency calculation, which show all real frequencies. Zero-point vibrational energies were added on the B3LYP frequency calculations (unscaled) using the same basis set as in the geometry optimizations. The electronic structure of **1** and **2** were examined by NBO analysis[59] as implemented in the Gaussian 03 package. A detailed conformational search for the molecules **1** and **2** was performed using DFT calculations to find the minimum energy of the highest stable conformer, and the geometry of this conformer was fully optimized applying the DFT method in aqueous phase (Figure 1). Because in physiological pH the predominant form of **1** is the *trans*-$[Ru(Bz)(NH_3)_4SO_3]$ species, all the calculations were performed considering L in **1** as a SO_3^{2-} ligand, except when mentioned in text. Solvation energies have been calculated using the polarizable continuum model (PCM).[60−62] The PCM is based on a description of the solvent as macroscopic continuum medium having suitable properties (dielectric constant, thermal expansion coefficient, etc.). In this procedure, the solute is embedded in a cavity in the dielectric medium defined above. The solute−solvent interactions are described in terms of the reaction field due to the presence of the dielectric medium, which acts as a perturbation on the Hamiltonian of the solute through its reaction potential. Single-point calculations with the B3LYP and the standard 6-311+G(d,p) basis sets for H, C, N, S, and O, and the LANL2DZ basis set for Ru was calculated. A dielectric constant of $\varepsilon = 78.39$ was used for the reference reaction of **1** and **2** in water. Vibrational frequencies were calculated from analytic second derivatives to check the minimum on the potential energy surface.

Parasites. The Y strain of *T. cruzi*, a partially Bz-resistant and highly virulent strain,[11] was used for all experiments. Swiss mice were infected intraperitoneally with 1.0×10^3 bloodstream trypomastigote forms of *T. cruzi* (BT) obtained from an intermediary strain-matched infected mouse. Before infection of intermediary mice, parasites were grown in Schneider's medium and purified from a monkey kidney fibroblast cell line LLC-MK2.

Evaluation of the Antiproliferative and Trypanocidal Activities in Vitro. All the experiments against trypomastigotes and epimastigotes were performed according to previous report.[18,36] BT were obtained from mice on the parasitemia peak and resuspended to 1.0×10^6/mL. Epimastigote forms (EF) were grown in a Schneider's medium, supplemented with 20% fetal calf serum, harvested during the exponential phase of growth, washed in phosphate-buffered saline (PBS), and resuspended to 2.0×10^6 parasites/mL. Then 200 μL of parasites were plated in triplicate onto 96-well microplates and treated with both **1** and **2** diluted in PBS (0.1, 0.25, 0.5, and 1.0 mM) and incubated at 37 °C, 5% CO_2. The parasite viability was subsequently assayed by determining the number motile forms in a hemocytometer. The percentage of trypanocidal activity (% TA) and the percentage of antiproliferative activity (growth inhibition, % GI) for both compounds **1** and **2** were calculated as follows: $\%\ TA = [1 - (L_{Dt}/L_{Ct})] \times 100$ and $\%\ GI = \{1 - [(L_{Dt} - L_{Df0})/L_{Ct} - L_{Cf0})]\} \times 100$, where L_{Dt} is the average of the number motile forms in a well containing the drug at time t, L_{Df0} is the average of the number motile forms in well containing the drug at time t = zero, L_{Ct} is the average of the number of motile forms in well in the absence of any compound at time t (negative control), and L_{Cf0} is the average of the number of motile forms in well in the absence of any compound at time t = zero.[36] The compound concentration corresponding to 50% of the antiproliferative or trypanocidal activities was later expressed as IC_{50epi} and $IC_{50try,}$ respectively.[36]

Evaluation of the Trypanocidal Activity in Vivo (Acute Models). Female Swiss mice, 5−6 weeks old, were bred and maintained under standard conditions in the animal house of the Department of Biochemistry and Immunology, School of Medicine of Ribeirão Preto-USP (Ribeirão Preto, Brazil). These animals were infected by intraperitoneal administration of 1.0×10^3 BT per mouse and treated with the doses of **1** at 100 nmol/kg/day = 85 μg/kg/day or at 385 nmol/kg/day = 330 μg/kg/day for 15 consecutive days (protocol A) or for only three days, the fifth, sixth, and seventh days that precede the parasitaemic peak (protocol B). Two other groups were treated with **2** at 385 μmol/kg/day = 100 mg/kg/day or at 100 nmol/kg/day = 26 μg/kg/day. Nontreated infected mice or infected mice treated only with PBS were used as control. In a model, compounds **1** and **2** were injected by intraperitoneal administration in 100 μL of PBS. In a second model, the doses of **1** and **2** (**2** dissolved in water containing gum arabic) were given by oral administration in 100 or 200 μL of PBS. All procedures performed in the studies described herein were approved by the Ethics Committee on Animal Research of the University of São Paulo. Moreover, it is committed to the 3R principle (replacement, reduction, refinement), in which alternative methods to the use of animals and the refinement of technicians aiming to diminish, whenever possible, the suffering and the number of animals in the project are proposed.[63,64] The course of infection was monitored by counting the number of motile trypomastigotes in 5 μL blood samples drawn from the tail veins, as previously described.[65]

Histological Analysis. All the untreated infected mice died of acute ChD 15−30 days postinfection and were immediately necropsied.[30] The majority of the treated mice survived infection and were euthanized 15 days after infection with *T. cruzi*. Hearts, livers, and skeletal muscles were fixed in 10% formaldehyde solution in PBS, embedded in paraffin, sectioned, stained with hematoxylin-eosin, and examined through light microscopy analysis.

Unspecific Cytotoxicity. In Vitro. Cell viability assay was performed on $CD11c^-$ $CD11b^+$ bone marrow-derived macrophages by propidium iodide (PI) exclusion as described elsewhere.[66,67] Briefly, after 24 h of incubation of 1×10^6 cells per cm^2 in 48-well culture plates (Costar) containing RuBz (0.1 to 1 mM concentrations) or RPMI medium alone, cells were harvested in separate assay tubes, adding PI (Sigma P 4170) to each tube (50 μM final concentration), and the cells were kept in the dark at room temperature for 15 min. After that, the cells were analyzed by fluorescence with a FACS Canto II cytometry system (BD biosciences). The total of cells acquired for each sample was 10000. Analysis was performed in FL2-A units. Background readings were obtained from cells incubated with RPMI medium alone and stained with PI. Positive controls were obtained by incubating cells with seriate dilutions of Triton (X-100) for 15 min before PI addition. The frequency of PI positive cells was determined according to these controls. Additionally, cell viability and proliferation was also evaluated using spleen cells from two Balb/c mice. This cells were cultured with different concentrations of **1** (10 nM up to 1 mM) or medium, and 6, 12, 24, and 48 h later, the percentage of viable cells were determined in an hemocytometer using trypan blue staining for exclusion (dead cells).[31] In another assay, spleen cells from two Balb/c mice were stained with CFSE (Sigma 5 μM) and cultured for 72 h on a 96-well plate (Nunc, 5.0×10^5 cells/well), under the same concentrations of **1** or medium. A set of wells was also added with ConA (2 μg/mL), for induction of nonspecific (policlonal) proliferation. After this, the cells suspensions were acquired in a FACscan flow cytometer and analyzed with Cellquest software (both Becton-Dickinson Immunocytometry Systems Inc., San Jose, CA).[32]

In Vivo. Swiss female mice (5- to 6-week-old) were treated with **1** diluted in PBS following the *up-and-down* test protocol for acute toxicity testing.[30] The compound was intraperitoneally administrated in a single dose to only one animal and a 48 h observation period followed. If death occurred, another animal would be chosen and would receive $^1/_3$ of the previous dose; if not, the next animal would receive three times the previous dose.[30] In this study the starting concentration was 100 μmol/kg.

Statistical Analysis. All the results herein presented were considered statistically significant ($P > 0.05$) and were expressed as mean ± sem The Mann−Whitney and Kruskal−Wallis were used to determine the statistical significance of the intergroup comparison.

Acknowledgment. We acknowledge the financial support from Coordenação de Aperfeiçoamento de Pessoal de Nível Superior (CAPES), the Millennium Institute for Vaccine Development and Technology (MIVDT/CNPq), Conselho Nacional de Desenvolvimento Científico e Tecnológico (CNPq), and Fundação de Amparo à Pesquisa do Estado de São Paulo (FAPESP).

Supporting Information Available: Combustion analyses for target compounds, parasitemia of Swiss mice infected with *T. cruzi* and treated with a single dose of **1** or **2**, characters and energies of LUMOs and HOMOs for complex **1**, Vero cells infected with *T. cruzi* and treated with **1** and **2** compounds. This material is available free of charge via the Internet at http://pubs.acs.org.

References

(1) Engels, D.; Savioli, L. Reconsidering the Underestimated Burden Caused by Neglected Tropical Diseases. *Trends Parasitol.* **2006**, *22*, 363–366.
(2) Centers for Disease Control and Prevention. Blood Donor Screening for Chagas Disease-United States 2006−2007. *MMWR Morbidity and Mortality Weekly Report* **2007**, *56*, 141−143.
(3) Reesink, H. W. European Strategies Against the Parasite Transfusion Risk Risque Parasitaire, Quelles Stratégies en Europe. *Trans. Clin. Biol.* **2004**, *12*, 1–4.
(4) Cerecetto, H.; González, M. Chemotherapy of Chagas' Disease: Status and New Development. *Curr. Top. Med. Chem.* **2002**, *2*, 1187–1213.
(5) Sajid, M.; McKerrow, J. H. Cysteine Proteases of Parasitic Organisms. *Mol. Biochem. Parasitol.* **2002**, *120*, 1–21.
(6) Docampo, R. Recent Developments in the Chemotherapy of Chagas' disease. *Curr. Pharm. Des.* **2001**, *7*, 1157–1164.
(7) Boiani, M.; Boiani, L.; Denicola, A.; de Ortiz, S. T.; Serna, E.; de Bilbao, N. V.; Sanabria, L.; Yaluff, G.; Nakayama, H.; de Arias, A. R.; Veja, C.; Rolan, M.; Gomez-Barrio, A.; Cerecetto, H.; González, M. 2*H*-Benzimidazole 1,3-Dioxide Derivatives: A New Family of Water-Soluble Anti-trypanosomatid Agents. *J. Med. Chem.* **2006**, *49*, 3215–3224.
(8) Buschini, A.; Giordani, F.; Albuquerque, C. N.; Pellacani, C.; Pelosi, G.; Rossi, C.; Zucchi, T. M.; Poli, P. Trypanocidal Nitroimidazole Derivatives: Relationships Among Chemical Structure and Genotoxic Activity. *Biochem. Pharmacol.* **2007**, *73*, 1537–1547.
(9) Maya, J. D.; Cassels, B. K.; Iturriaga-Vásquez, P.; Ferreira, J.; Faúndez, M.; Galanti, N.; Morello, A. Mode of Action of Natural and Synthetic Drugs Against *Trypanosoma cruzi* and their Interaction with the Mammalian Host. *Comp. Biochem. Physiol.* **2007**, *146*, 601–620.
(10) Castro, J. A.; Meca, M. M.; Bartel, L. C. Toxic Side Effect of Drugs Used to Treat Chagas' Disease (American trypanosomiasis). *Human. Exp. Toxicol.* **2006**, *25*, 471–479.
(11) Martinez-Díaz, R. A.; Escario, J. A.; Nogal-Ruiz, J. J.; Gómez-Barrio, A. Biological Characterization of *Trypanosoma cruzi* Strains. *Mem. Inst. Oswaldo Cruz* **2001**, *96*, 53–59.
(12) Sanchez-Delgado, R. A.; Anzellotti, A. Metal Complexes as Chemotherapeutic Agents Against Tropical Diseases: Trypanosomiasis, Malaria and Leishmaniasis. *Mini. Rev. Med. Chem.* **2004**, *4*, 23–30.
(13) Otero, L.; Vieites, M.; Bioani, L.; Denicola, A.; Rigol, C.; Opazo, L.; Olea-Azar, C.; Maya, J. D.; Morello, A.; Krauth-Siegel, R. L.; Piro, O. E.; Castellano, E.; González, M.; Gambino, D.; Cerecetto, H. Novel Antrypanosomal Agents Based on Palladium Nitrofurylthiosemicarbazone Complexes: DNA and Redox Metabolism as Potential Therapeutic Targets. *J. Med. Chem.* **2006**, *49*, 3322–3331.
(14) Sánchez-Delgado, R. A.; Navarro, M.; Lazardi, K.; Atencio, R.; Capparelli, M.; Vargas, F.; Urbina, J. A.; Bouillez, A.; Noels, A. F.; Mais, D. Toward a Novel Metal-Based Chemotherapy Against Tropical Diseases. Part 4. Synthesis and Characterization of New Metal−Clotrimazole Complexes and Evaluation of Their Activity Against *Trypanosoma cruzi*. *Inorg. Chim. Acta.* **1998**, 528–540.
(15) Navarro, M.; Lahmann, T.; Cisneros-Fajardo, E. J.; Fuentes, A.; Sánchez-Delgado, R. A.; Silva, P.; Urbina, J. A. Toward a Novel Metal-Based Chemotherapy Against Tropical Diseases. Part 5. Synthesis and Characterization of New Ru(II) and Ru(III) Clotrimazole and Ketoconazole Complexes and Evaluation of Their Activity Against *Trypanosoma cruzi*. *Polyhedron* **2000**, *19*, 2319–2325.
(16) Tfouni, E.; Krieger, M.; McGarvey, B.; Franco, D. W. Structure, Chemical and Photochemical Reactivity and Biological Activity of Some Ruthenium Nitrosyl Complexes. *Coord. Chem. Rev.* **2003**, *236*, 57–69.
(17) Silva, J. J. N.; Osakabe, A. L.; Pavanelli, W. R.; Silva, J. S.; Franco, D. W. In Vitro and in Vivo Antiproliferative and Trypanocidal Activities of Ruthenium NO Donors. *Br. J. Pharmacol.* **2007**, *152*, 112–121.
(18) Vespa, G. N. R.; Cunha, F. Q.; Silva, J. S. Nitric Oxide is Involved in Control of *Trypanosoma cruzi*-Induced Parasitemia and Direct Kills of the Parasite in vitro. *Infect. Immun.* **1994**, *62*, 5177–5182.
(19) Isied, S. S.; Taube, H. Effects of Sulfur Dioxide, Bisulfite(1−), and Sulfite(2−) as Auxiliary Ligands on the Reactivity of Ammineruthenium(II)−ligand Bonds. *Inorg. Chem.* **1974**, *13*, 1545–1551.
(20) Brown, G. M.; Sutton, J. E.; Taube, H. Binding of a Tetraammineruthenium Complex to Imidazole and Purine Derivatives under Equilibrium Conditions. *J. Am. Chem. Soc.* **1978**, *26*, 2767–2774.
(21) Borges, S. S. S.; Davanzo, C. U.; Castellano, E. E.; Z-Zchpector, J.; Silva, S. C.; Franco, D. W. Ruthenium Nitrosyl Complexes with N-heterocyclic Ligands. *Inorg. Chem.* **1998**, *37*, 2670–2677.
(22) Maya, J. D.; Bollo, S.; Nuñez-Vergara, L. J.; Squella, J. A.; Repetto, Y.; Morello, A.; Périé, J.; Chauvière, G. *Trypanosoma cruzi*: Effect and Mode of Action of Nitroimidazole and Nitrofuran Derivatives. *Biochem. Pharmacol.* **2003**, *65*, 999–1006.
(23) Matsubara, T.; Ford, P. Some Applications of Cyclic Voltammetry to the Reactions and Properties of Ruthenium Ammine Complexes. Reduction Potentials and Rate Studies. *Inorg. Chem.* **1976**, *15*, 1107–1110.
(24) Bollo, S.; Núñez-Vergara, L. J.; Bontá, M.; Chauviere, G.; Périé, J.; Squella, J. A. Cyclic Voltammetric Studies on Nitro Radical Anion Formation From Megazol and Some Related Nitroimidazole Derivatives. *J. Electroanal. Chem.* **2001**, *511*, 46–54.
(25) Toledo, J. C.; Lima Neto, B. S.; Franco, D. W. Mutual Effects in the Chemical Properties of the Ruthenium Metal Center and Ancillary Ligands upon Coordination. *Coord. Chem. Rev.* **2005**, *249*, 419–431.
(26) Clarke, M. J.; Taube, H. Pentaammineruthenium−guanine Complexes. *J. Am. Chem. Soc.* **1974**, *96*, 5413–5419.
(27) Franco, D. W.; Taube, H. Triethyl Phosphite as a Ligand on Ruthenium(II). *Inorg. Chem.* **1978**, *17*, 571–578.
(28) Vogt, L. H.; Katz, J. L.; Wiberley, S. E. The Crystal and Molecular Structure of Ruthenium−Sulfur Dioxide Coordination Compounds. I. Chlorotetraammine(Sulfur Dioxide)Ruthenium(II) Chloride. *Inorg. Chem.* **1965**, *4*, 1157–1163.
(29) Nothenberg, M. S.; Takeda, G. K. F.; Najjar, R. Adducts of Nitroimidazoles Derivatives with Rhodium(II) Carboxylates: Synthesis, Characterization, and Evaluation of Antichagassic Activities. *J. Inorg. Biochem.* **1991**, *42*, 217–229.
(30) Lamas, M. C.; Villaggi, L.; Nocito, I.; Bassani, G.; Leonardi, D.; Pascutti, F.; Serra, E.; Salomón, C. J. Development of Parenteral Formulations and Evaluation of the Biological Activity of the Trypanocide Drug Benznidazole. *Int. J. Pharm.* **2006**, *307*, 239–243.
(31) Freshney, R. *Culture of Animal Cells: A Manual of Basic Technique*; Alan R. Liss, Inc.: New York, 1987, pp 117.
(32) Lyons, A. B.; Parish, C. R. Determination of Lymphocyte Division by Flow Cytometry. *J. Immunol. Methods* **1994**, *171*, 131–137.
(33) Melo, P. S.; Durán, N.; Haun, M. Cytotoxicity of Prodigiosin and Benznidazole on V79 Cells. *Toxicol. Lett.* **2000**, *116*, 237–242.
(34) Bruce, R. D. An Up-and-Down Procedure For Acute Toxicity Testing. *Fundam. Appl. Toxicol.* **1985**, *5*, 151–157.
(35) Castro, S. L.; Meirelles, M. N. L. Effect of Drugs on *Trypanosoma cruzi* and on its Interaction with Heart Muscle Cell in Vitro. *Mem. Inst. Oswaldo Cruz* **1986**, *82*, 209–218.
(36) Silva, J. J. N.; Pavanelli, W. R.; Silva, J. S.; Franco, D. W. Experimental Chemotherapy Against *Trypanosoma cruzi* Infection Using Ruthenium NO-donors. *Antimicrob. Agents Chemother.* **2007**, . submitted.
(37) Silva, R. S. F.; Costa, E. M.; Trindade, U. L. T.; Teixeira, D. V.; Pinto, M. C. F. R.; Santos, G. L.; Malta, V. R. S.; De Simone, C. A.; Pinto, A. V.; De Castro, S. L. Synthesis of Naphthofuranquinones with Activity Against *Trypanosoma cruzi*. *Eur. J. Med. Chem.* **2006**, *41*, 526–530.
(38) Molina, J.; Martins-Filho, O.; Brener, Z.; Romanha, A. J.; Loebenberg, D.; Urbina, J. A. Activity of the Triazole Derivative SCH 56592 (Posaconazole) Against Drug-resistant Strains of the Protozoan Parasite *Trypanosoma* (*Schizotrypanum*) *cruzi* in Immunocompetent and Immunosuppressed Murine Hosts. *Antimicrob. Agents Chemother.* **2000**, *44*, 150–155.
(39) Ferraz, M. L.; Gazzinelli, R. T.; Alves, R. O.; Urbina, J. A.; Romanha, A. J. The Anti-*Trypanosoma cruzi* Activity of Posaconazole in a Murine Model of Acute Chagas' Disease is Less Dependent on Gamma Interferon Than That of Benznidazole. *Antimicrob. Agents Chemother.* **2007**, *51*, 1359–1364.

(40) Sanchez-Delgado, R.; Navarro, M.; Lazardi, K.; Atencio, R.; Capparelli, M.; Vargas, F.; Urbina, J. A.; Bouillez, A.; Noels, A. F.; Mais, D. Toward a Novel Metal Based Chemotherapy Against Tropical Disease 4. Synthesis and Characterization of a New Metal−Clotrimazole Complexes and Evaluation of Their Activity Against *Trypanosoma cruzi*. *Inorg. Chim. Acta* **1998**, *275*−*276*, 528–540.

(41) Otero, L.; Nobia, P.; Gambino, D.; Crecetto, H.; González, M.; Ellena, J. A.; Piro, O. E. Synthesis and Characterization of New Ruthenium Complexes with Active Ligands Against Chagas' Disease. *Inorg. Chim. Acta* **2003**, *344*, 85–94.

(42) Petray, P. B.; Morilla, M. J.; Corral, R. S.; Romero, E. L. In Vitro Activity of Etanidazole Against the Protozoan Parasite *Trypanosoma cruzi*. *Mem. Inst. Oswaldo Cruz* **2004**, *99*, 233–235.

(43) Squella, J. A.; Letelier, M. E.; Lindermeyer, L.; Nuñez-Vergara, L. J. Redox Behaviour of Nifuroxazide: Generation of the One-Electron Reduction Product. *Chem.*−*Biol. Interact.* **1996**, *99*, 227–238.

(44) Cerecetto, H.; Di Maio, R.; González, M.; Risso, M.; Sagrera, G.; Seoane, G.; Denicola, A.; Peluffo, G.; Quijano, C.; Stoppani, A.; Paulino, M.; Olea-Azar, C.; Basombrio, M. A. Synthesis and Antitrypanosomal Evaluation of *E*-isomers of 5-Nitro-2-furaldehyde and 5-Nitrothiophene-2-carboxaldehyde Semicarbazone Derivatives. Structure−Activity Relationships. *Eur. J. Med. Chem.* **2000**, *35*, 343–350.

(45) Dias, L. R. S.; Santo, M. B.; Albuquerque, S.; Castro, H. C.; Souza, A. M. T.; Freitas, A. C. C.; DiVaio, M. A. V.; Cabral, L. M.; Rodrigues, C. R. Synthesis, in Vitro Evaluation, and SAR Studies of a Potential Antichagasic 1*H*-Pyrazolo[3,4-*b*]pyridine Series. *Bioorg. Med. Chem.* **2007**, *15*, 211–219.

(46) Porcal, W.; Paola, H.; Aguire, G.; Bioani, L.; Bioani, M.; Merlino, A.; Ferreira, A.; Di Maio, R.; Castro, A.; González, M.; Cerecetto, H. Second Generation of 5-Ethenylbenzofuroxan Derivatives as Inhibitors of *Trypanosoma cruzi* Growth: Synthesis, Biological Evaluation, and Structure−Activity Relationships. *Bioorg. Med. Chem.* **2007**, *15*, 2768–2781.

(47) Marin-Neto, J. A.; Cunha-Neto, E.; Maciel, B. C.; Simões, M. V. Phatogenesis of Chronic Chagas' Heart Disease. *Circulation.* **2007**, *115*, 1109–1123.

(48) Garcia, S.; Ramos, C. O.; Senra, J. F.; Vilas-Boas, F.; Rodrigues, M. M.; Campos-de-Carvalho, A. C.; Ribeiro-Dos-Santos, R.; Soares, M. B. Treatment with Benznidazole During the Chronic Phase of Experimental Chagas' Disease Decreases Cardiac Alterations. *Antimicrob. Agents Chemother.* **2005**, *49*, 1521–1528.

(49) Perrin, D. D.; Armarego, W. L. F.; Perrin, D. R. *Purification of Laboratory Chemicals*; Pergamon Press: Elmsford, NY, 1980.

(50) Shriver, D. F. *The Manipulation of Air-Sensitive Compound*. McGraw-Hill: New York, 1969.

(51) Clarke, M. J. Electrochemistry, Synthesis, and Spectra of Pentaammineruthenium(III) Complexes of Cytidine, Adenosine, and Related Ligands. *J. Am. Chem. Soc.* **1978**, *100*, 5068–5075.

(52) Galia, E.; Nicolaides, E.; Horter, D.; Lobenberg, R.; Reppas, C.; Dressman, J. B. Evaluation of Various Dissolution Media for Predicting In Vivo Performance of Class I and II Drugs. *Pharm. Res.* **1998**, *15*, 698–705.

(53) Kasim, N. A.; Whitehouse, M.; Ramachandran, C.; Bermejo, M.; Lennernäs, H.; Hussain, A. S.; Jungiger, H. E.; Stavchansky, S. A.; Midha, K. K.; Shah, V. P.; Amidon, G. L. Molecular Properties of WHO Essential Drugs and Provisional Biopharmaceutical Classification. *Mol. Pharm.* **2004**, *1*, 85–96.

(54) Frisch, M. J.; Trucks, G. W.; Schlegel, H. B.; Scuseria, G. E.; Robb, M. A.; Cheeseman, J. R.; Montgomery, J. A., Jr.; Vreven, T.; Kudin, K. N.; Burant, J. C.; Millam, J. M.; Iyengar, S. S.; Tomasi, J.; Barone, V.; Mennucci, B.; Cossi, M.; Scalmani, G.; Rega, N.; Petersson, G. A.; Nakatsuji, H.; Hada, M.; Ehara, M.; Toyota, K.; Fukuda, R.; Hasegawa, J.; Ishida, M.; Nakajima, T.; Honda, Y.; Kitao, O.; Nakai, H.; Klene, M.; Li, X.; Knox, J. E.; Hratchian, H. P.; Cross, J. B.; Bakken, V.; Adamo, C.; Jaramillo, J.; Gomperts, R.; Stratmann, R. E.; Yazyev, O.; Austin, A. J.; Cammi, R.; Pomelli, C.; Ochterski, J. W.; Ayala, P. Y.; Morokuma, K.; Voth, G. A.; Salvador, P.; Dannenberg, J. J.; Zakrzewski, V. G.; Dapprich, S.; Daniels, A. D.; Strain, M. C.; Farkas, O.; Malick, D. K.; Rabuck, A. D.; Raghavachari, K.; Foresman, J. B.; Ortiz, J. V.; Cui, Q.; Baboul, A. G.; Clifford, S.; Cioslowski, J.; Stefanov, B. B.; Liu, G.; Liashenko, A.; Piskorz, P.; Komaromi, I.; Martin, R. L.; Fox, D. J.; Keith, T.; Al-Laham, M. A.; Peng, C. Y.; Nanayakkara, A.; Challacombe, M.; Gill, P. M. W.; Johnson, B.; Chen, W.; Wong, M. W.; Gonzalez, C.; Pople, J. A. Gaussian 03, revision C.02; Gaussian, Inc.: Wallingford, CT, 2004.

(55) Becke, A. D. Density-Functional Thermochemistry. III. The Role of Exact Exchange. *J. Chem. Phys.* **1993**, *98*, 5648–5652.

(56) Lee, C.; Yang, W.; Parr, R. G. Development of the Colle−Salvetti Correlation-Energy Formula into a Functional of the Electron Density. *Phys. Rev. B* **1988**, *37*, 785–789.

(57) Farkas, O.; Schlegel, H. B. Methods for Optimizing Large Molecules. II. Quadratic Search. *J. Chem. Phys.* **1999**, *111*, 10806–10814.

(58) Becke, A. D. Density-Functional Exchange-Energy Approximation with Correct Asymptotic Behavior. *Phys. Rev. A* **1988**, *38*, 3098–3100.

(59) Glendening, E. D.; Badenhoop, J. K.; Reed, A. E.; Carpenter, J. E.; Bohmann, J. A.; Morales, C. M.; Weinhold, F. *NBO 3.0*; Theoretical Chemistry Institute: Madison, WI, 1998.

(60) Cances, E.; Mennucci, B.; Tomasi, J. A New Integral Equation Formalism for the Polarizable Continuum Model: Theoretical Background and Applications to Isotropic and Anisotropic Dielectrics. *J. Chem. Phys.* **1997**, *107*, 3032–3041.

(61) Miertus, S.; Scrocco, E.; Tomasi, J. Electrostatic Interaction of a Solute with a Continuum. A Direct Utilization of ab Initio Molecular Potentials for the Prevision of Solvent Effects. *Chem. Phys.* **1981**, *55*, 117–129.

(62) Foresman, J. B.; Frisch, A. E. *Exploring Chemistry With Electronic Structure Methods*; Gaussian, Inc.: Pittsburgh, PA, 1998.

(63) Zimmermann, M. Ethical Guidelines for Investigations of Experimental Pain in Conscious Animals. *Pain* **1983**, *16*, 109–110.

(64) Russell, W. M. S.; Burch, R. L. The Principles of Humane Experimental Technique; Hyperion Books: New York, 1992.

(65) Brener, Z. Therapeutic Activity and Criterion of Cure on Mice Experimentally Infected with *Trypanosoma cruzi*. *Rev. Inst. Med. Trop.* **1962**, *4*, 389–396.

(66) Cunnick, J.; Kaur, P.; Cho, Y.; Groffen, J.; Heisterkamp, N. Use of Bone Marrow-Derived Macrophages to Model Murine Innate Immune Responses. *J. Immunol. Methods* **2006**, *311*, 96–105.

(67) Coder, D. M. Assessment of Cell Viability. In *Current Protocols in Cytometry*; Robinson, J. P., Ed.; International Society for Analytical Cytology: Bethesda, MD, 2008; pp 447−458.

JM701306R